Chapter-5. Surface Potential Based Current Model for an OTFT

5.1 INTRODUCTION

This chapter[3], deals with the modeling aspects of an OTFT. Due to rapid progress in material processing technology and dedicated efforts from researchers: both from industry and academic, performance of an OTFT, in terms of mobility, subthreshold swing, I_{ON}/I_{OFF} ratio and stability have seen a significant improvement. However, a reliable compact model which could describe the I-V characteristics of OTFTs is still missing and needs to be addressed. Conventional device models, available as a part of the commercial computer aided design (CAD) tools are tailored for inorganic semiconductors, especially silicon. Such models, developed with primary focus on silicon doesn't fit for organic semiconductors (OSCs). They poorly replicate the observed characteristics of an OTFT. Hence, there is an urgent need to develop an accurate, computational efficient and a physics based model for OTFTs.

Organic Semiconductors, both small molecules as well as polymer can be classified as dis-ordered semiconductors. The weak van der Waals forces among the molecules result in severe localization of the energy states. Hence, in OSCs, energy gap between Highest Occupied Molecular Orbital (HOMO) and Lowest Unoccupied Molecular Orbital (LUMO) is filled with unwanted electronic states: referred as traps. These trap states, play a significant role in the conduction mechanism of OSCs. Trap states, can be classified as deep states and tail states based on their location with reference to the fermi level. Those states which lie a few kT (k is the Boltzmann constant and T is absolute temperature) away from the HOMO/LUMO edge are classified as tail states while, those which lie far away from the HOMO/LUMO band

[3] This chapter in its similar form has been published as "Surface potential based current model for organic thin film transistor considering double exponential density of states." K.B.R.Teja, N.Gupta, *Superlattices and Microstructures* 142 (2020): 106513.

edge and close to the intrinsic fermi level are classified as deep states. Understanding the exact location and density of trap states is essential to assess the conductivity of OSCs. Several models have been proposed in the literature to model trap states in OSCs [33], [82], [86], [159]. These models explain the distribution of trap states in OSCs and referred as density of states (DoS). Among, various DoS models available, double exponential and Gaussian are most commonly used models for OTFTs [160]–[162]. To the best of our knowledge, no conclusive evidence has been drawn on which of these models fit the best. The quest to find one such DoS model which could explain the characteristics of an OTFT is in progress. However, in this work we choose the double exponential DoS model, which is reported by several researchers as the best fit model for an OTFT.

Transistor models can be broadly classified as: (i) Threshold voltage (V_T) based models, (ii) inversion charge based models and (iii) surface potential based models [89][163]. V_T based models are well studied models and preferred by circuit designers due to their direct correspondence to circuit design and optimization. Although, V_T based models are well studied and established in case of inorganic MOSFETs, they can't be readily adapted for OTFTs. The challenges for adapting V_T based models for an OTFT include: defining V_T and extracting V_T. Since, an OTFT operates in accumulation mode, defining threshold voltage is a challenge. Moreover, extracting V_T from I-V characteristics is even more challenging. This is due to the large sub-threshold swing in OTFTs. Furthermore, the V_T extraction procedures available in the literature rely on a large number of fitting parameters like contact resistance, gate voltage and field dependence of mobility. Extraction of these fitting parameters is not only a complex process but also inappropriate for physics based models due to their empirical nature. The other alternative, inversion charge based models are not applicable for accumulation mode. Moreover, inversion charge based models cannot explain certain important electrical characteristics which include: noise, gate current partition in the channel [164].

Owing to the non-adaptability of V_T based model and inversion charge based models, surface potential based models have gained significant attention for OTFTs.

Unlike V_T based models, surface potential based models are developed from fundamental device physics and uses little or no empirical constants. Therefore, device characteristics obtained using surface potential based models could be related directly to the intrinsic material properties of device. Therefore, provides a better insight into the correlation between performance parameters of an OTFT and intrinsic material properties. Hence, surface potential based models are best suited for OTFTs. They provide accurate, reliable and physics based models for obtaining device characteristics of OTFT. However, a major challenge while adapting surface potential is its computation which is explained further in next section. The main objective of the current work is to address the problem of computing surface potential and to develop an efficient and accurate model for surface potential which can be incorporated to develop models for an OTFT.

The remaining portion of this chapter is organized as follows: Section-5.2 explains various DoS models and the concept surface potential in OTFTs. Section-5.3, presents an analytical expression for surface potential considering double exponential DoS. Section-5.4, compares the results obtained from analytical expression against numerical simulation. Followed by, I-V characteristics of an OTFT obtained using the analytical expression derived in Section-5.3. Section-5.5 summarizes the work and presents a conclusion.

5.2 TRAP STATES DISTRIBUTION AND SURFACE POTENTIAL

Organic semiconductors, both small molecule as well as polymers can be categorized as energetically disordered. In such materials, the charge transport mechanism is determined by the localized trap states in the band gap between HOMO LUMO. The energetic disorder can be attributed to presence of interface dipole, weak molecular interactions among the polymer molecules, orientation of the polymer side chains and grain boundaries. Though the disorder is an intrinsic parameter of the OSCs, it is also strongly influenced by the deposition technique, temperature and the interface

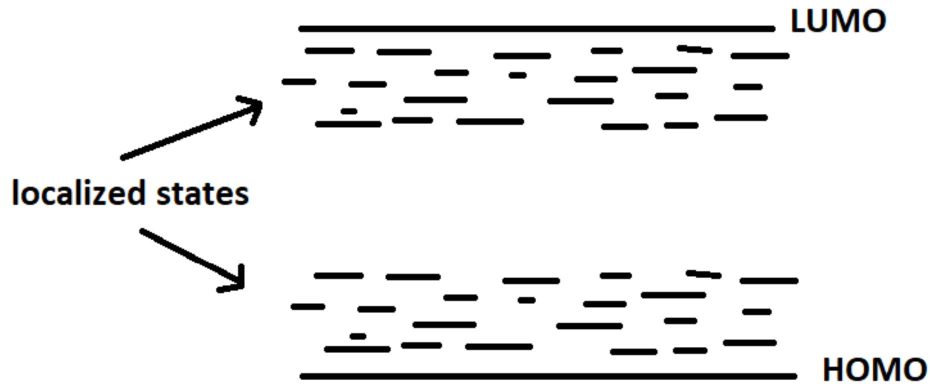

Figure 5-1 Lowest unoccupied molecular orbital (LUMO), highest occupied molecular orbital (HOMO) and localized states in an organic semiconductor

materials like contacts, substrate and gate dielectric. A schematic representation of energy band diagram of such energetic disordered OSC material is shown in Fig.5-1.

The distribution of localized trap states between HOMO and LUMO is expressed in the form of density of states. DoS is the number of energy states available per unit volume per energy level. The actual nature of DoS in organic semiconductors is still a debated topic and several models have been proposed by various research groups [82][85], [159]. A closer examination of various models presented for OSCs suggests that organic semiconducting material: single crystalline or amorphous in its doped or un-doped form can be modeled using either a Gaussian distribution or an exponential distribution and sometimes even the summation of the two [161]. Tail states, the ones which are close to the HOMO/LUMO can be accurately modeled either by a Gaussian distribution or an exponential distribution. While, deep states: which lie away from HOMO/LUMO edges, can be described well using an exponential distribution. Hence, a better approximation for localized trap distribution in an OSC which includes both the tail states and deep states is a double exponential density of states given as [161]:

$$g(E) = \frac{N_{Deep}}{\phi_{Deep}} \exp\left(\frac{E - E_{LUMO}}{\phi_{Deep}}\right) + \frac{N_{Tail}}{\phi_{Tail}} \exp\left(\frac{E - E_{LUMO}}{\phi_{Tail}}\right) \tag{5.1}$$

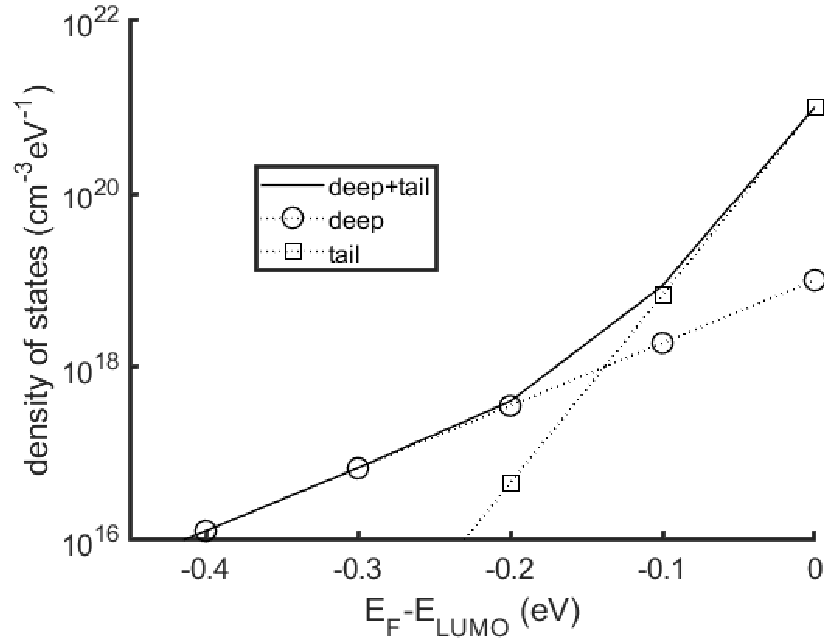

Figure 5-2 Double exponential density of states (DoS) distribution in an organic semiconductor. Plot shown for the case: N_{Deep}=10^{19} $cm^{-3}eV^{-1}$, N_{Tail}=10^{21} $cm^{-3}eV^{-1}$, ϕ_{Tail} =20 meV, ϕ_{Deep}=60 meV

where, *g(E)* is the density of states, N_{Deep} and N_{Tail} are concentration of deep and tail states per unit volume. ϕ_{Deep} and ϕ_{Tail} are the characteristic energy of deep and tail states. E_{LUMO} is the LUMO edge. DoS stated in Eq.(5.1) is for n-type OTFTs; in which, drain current is determined by acceptor trap states [165]. A similar distribution can also be stated for p-type OTFTs. Fig.5-2 shows trap state distribution for a n-type OTFT. It could be observed that deep states dominate the distribution when the fermi level E_F is close to the mid gap while tail states dominate when E_F moves close to the band edge. This is a significant observation, and will be used later in developing analytical solution for surface potential.

Surface potential is defined as the potential at gate dielectric/channel interface. It is usually evaluated using the gradual channel approximation (GCA). GCA, neglects the electric field along the lateral direction. As a result, Poisson equation at the gate dielectric/channel interface becomes 1-D. The resultant expression is shown in Eq.(5.2). Surface potential in the energy band diagram of a MOS structure comprising

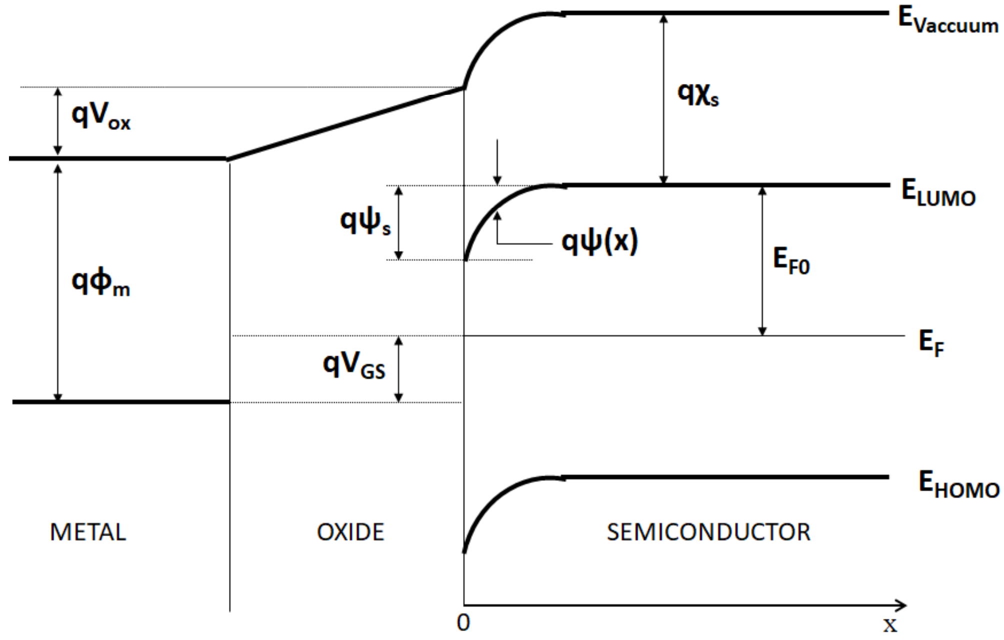

Figure 5-3 Energy band diagram of a metal-oxide-semiconductor structure showing various potentials and energy levels, metal work function ($q\Phi_M$) and electron affinity of the semiconductor ($q\chi_S$)

of OSC is shown in Fig.5-3. Generalized 2-D Poisson equation at the gate dielectric/channel interface is given by[161], [165], [166]

$$\nabla^2\psi = -\left(\frac{\partial F_x}{\partial x} + \frac{\partial F_y}{\partial y}\right) = \frac{q}{\varepsilon_{osc}}\left(N_D^- + N_T^- + n_{free}\right) \tag{5.2}$$

where, ψ is the surface potential, F_x, F_y are the electric field components in x, y direction respectively

Using, gradual channel approximation (GCA) (which is very well valid in the case of long channel OTFTs), which states that $F_x >> F_y$. N_D^-, N_T^- denote the ionized trapped carrier concentration in the deep states and tail states respectively. n_{free} denotes free carrier concentration. In, organic semiconductors, most of the charge carried are trapped in the trap states ($N_D^- + N_T^- >> n_{free}$) which is also the reason why they exhibit low conductivity. Using, above two condition, Poisson's equation can be reduced to

$$\frac{d^2\psi}{dx^2} = -\frac{\partial F_x}{\partial x} = \frac{q}{\varepsilon_{osc}}\left(N_D^- + N_T^-\right) \tag{5.3}$$

The electric field can be obtained as shown below [165]

$$F_x(\psi, V_{ch}) = \frac{d\psi}{dx} = \sqrt{2\int_0^{\psi}\left(\frac{d^2\psi}{dx^2}\right)d\psi} \tag{5.4}$$

where, V_{ch} is the channel potential.

According to Gauss's Law, charge accumulated near the gate dielectric/channel interface in terms of electric field is given by [161], [165], [167], [168]

$$\varepsilon_{osc}F_x(\psi, V_{ch}) = C_i(V_{GS} - V_{FB} - \psi) \tag{5.5}$$

where, ε_{osc} is the dielectric constant of the organic semiconductor, C_i is the capacitance per unit area of the gate insulator, V_{GS} is the gate-source potential, V_{FB} is the flat band voltage.

Using Eq.(5.4) and Eq.(5.5) an expression for electric field can be obtained as: [161]

$$F_x = \sqrt{\frac{2q}{\varepsilon_{osc}}\left[N_{Deep}\phi_{Deep}\left(\exp\left(\frac{\psi - V_{ch}}{\phi_{Deep}}\right) - 1\right)\exp\left(-\frac{qE_{F0}}{\phi_{Deep}}\right) + N_{Tail}\phi_{Tail}\left(\exp\left(\frac{\psi - V_{ch}}{\phi_{Tail}}\right) - 1\right)\exp\left(-\frac{qE_{F0}}{\phi_{Tail}}\right)\right]} \tag{5.6}$$

Using the conditions: $\exp\left(\frac{\psi - V_{ch}}{\phi_{Deep}}\right) >> 1$ and $\exp\left(\frac{\psi - V_{ch}}{\phi_{Tail}}\right) >> 1$ Eq.(5.6) can be simplified as:

$$F_x \approx \sqrt{\frac{2q}{\varepsilon_{osc}}\left[N_{Deep}\phi_{Deep}\exp\left(\frac{\psi - V_{ch} - qE_{F0}}{\phi_{Deep}}\right) + N_{Tail}\phi_{Tail}\exp\left(\frac{\psi - V_{ch} - qE_{F0}}{\phi_{Tail}}\right)\right]} \tag{5.7}$$

Substituting Eq.(5.7) in Eq.(5.5)

$$(V_{GF} - \psi)^2 = X_{Deep}\exp\left(\frac{\psi - V_{ch}}{\phi_{Deep}}\right) + X_{Tail}\exp\left(\frac{\psi - V_{ch}}{\phi_{Tail}}\right) \tag{5.8}$$

$$X_{Deep} = \frac{2q\varepsilon_{OSC}N_{Deep}\phi_{Deep}}{C_i^2} \quad X_{Tail} = \frac{2q\varepsilon_{OSC}N_{Tail}\phi_{Tail}}{C_i^2} \tag{5.9}$$

where, $V_{GF} = V_{GS} - V_{FB}$

The equation in Eq.(5.8) is a non-linear transcendental expression and it is difficult to have a closed form expression without making approximations. It can be solved only using numerical solvers iteratively. However, iterative methods are suitable and used very frequently in device simulators. They don't fit well into circuit simulators. Since, circuit simulators have limited capabilities and can implement only

regular algebraic expressions. Hence there is a need to develop an accurate, non-iterative solution which could be incorporated into circuit simulators.

Several research groups have proposed various techniques to address the issue of non-iterative solution for obtaining surface potential by solving Eq.(5.8). The problem of calculating surface potential is similar for both OTFTs and amorphous oxide TFTs. Various techniques presented in the case of amorphous oxide TFTs include: a Lambert-W function based solution proposed by Wang et al.[36] and a second order Taylor series expansion combined with a correction term introduced by Schroder series by Zong et al.[166]. Colalongo [161] has proposed a solution using the Lagrange reversion theorem. He also proposed another technique based on Lambert-W function for calculating surface potential in InGaZnO thin film transistors [168]. Among these techniques, Lambert-W based approach is very accurate, however, it is not suitable for circuit simulators, since it is a special mathematical function which is not available in circuit simulators. A few other approaches proposed include algebraic approximations for Lambert-W function which introduces significant error, also they are multi-step processes and fit only for a certain region with errors shooting up beyond the region in which the approximation is valid. In case of multiple approximations for various regions they also necessitate the use of empirical smoothing function to ensure continuity of the solution. The technique proposed in section-5.3 for calculating surface potential uses a simple yet accurate technique to solve the problem.

5.3 AN EXPRESSION FOR SURFACE POTENTIAL

To obtain an expression for surface potential near the gate dielectric/channel interface in an OTFT, we need to solve Eq.(5.8). A close observation at Eq.(5.8) reveals that, left hand side (LHS) is a quadratic term while on the right hand side (RHS) is an exponential term. The exponential term on the RHS has ϕ_{Deep} and ϕ_{Tail} in the denominator which represent the characteristic energies of deep and tail states respectively. These parameters are typically in the order of a few meV. Hence, when V_{GF} is small (less than V_{ch}), surface potential is approximately equal to V_{GF}. In this case, the LHS is zero while the exponential terms on the RHS have a negative numerator

resulting in a very small value close to zero. Hence, a reasonable approximation for the surface potential is V_{GF}. From a physical perspective, when V_{GF} is low, there is little or no band bending near the interface. As V_{GF} raises in magnitude, bands near the gate dielectric/channel interface starts bending and surface potential follows V_{GF}. Once V_{GF} value increases beyond V_{ch}, surface potential saturates and attains a constant value, which results in surface potential, close to V_{ch}. The exact value can be calculated using the procedure discussed below.

Numerical methods for solving transcendental equations can be classified as (i) single starting variable and (ii) two starting variables. Single starting variable methods are preferred over two starting variables owing to ease of picking up an initial guess. Newton-Raphson method, is a single variable starting technique in which the solution of a transcendental equation $f(x)$ is obtained using the procedure shown below

$$x_{i+1} = x_i - \left.\frac{f(x)}{f'(x)}\right|_{x=x_i} \tag{5.10}$$

Where, i is the iteration, $f'(x)$ is the first derivative of $f(x)$. The process in Eq.(5.10) is repeated iteratively, until the results obtained in two consecutive iterations are almost equal. The term almost equal to zero is determined by a relative tolerance which is typically set as 10^{-6}. The number of iterations needed to obtain the solution is a measure of how good the numerical method and the initial guess are. In a few cases, the solution may not be possible because two consecutive values may not be close to each other even after a considerable number of iterations. This problem is referred as convergence problem in numerical solvers. Logarithmic functions are known to converge fast when compared to linear functions. Hence, surface potential expression in Eq.(5.8) is converted to logarithmic function as shown below

$$f(y) = 2\ln\left(V_{GF} - y - V_{ch}\right) - \ln\left(X_{Deep}\exp\left(\frac{y}{\phi_{Deep}}\right) + X_{Tail}\exp\left(\frac{y}{\phi_{Tail}}\right)\right) \tag{5.11}$$

where, $y = \psi - V_{ch}$ the first derivative of $f(y)$ is given below

$$f'(y) = \frac{-2}{V_{GF} - y - V_{ch}} - \frac{\dfrac{X_{Deep}}{\phi_{Deep}}\exp\left(\dfrac{y}{\phi_{Deep}}\right) + \dfrac{X_{Tail}}{\phi_{Tail}}\exp\left(\dfrac{y}{\phi_{Tail}}\right)}{X_{Deep}\exp\left(\dfrac{y}{\phi_{Deep}}\right) + X_{Tail}\exp\left(\dfrac{y}{\phi_{Tail}}\right)} \tag{5.12}$$

Using Eq.(5.11) and Eq.(5.12) in Eq.(5.10) the first iterative solution for $f(y)$ expressed as y_1 in terms of the initial guess y_0 is given as

$$y_1 = y_0 - \left.\frac{f(y)}{f'(y)}\right|_{y=y_0} \tag{5.13}$$

substituting the expression and using the initial condition, $y_0 = 0$, surface potential is given by

$$\psi = V_{ch} + \frac{2\ln\left(V_{GF} - V_{ch}\right) - \ln\left(X_{Deep} + X_{Tail}\right)}{\dfrac{2}{V_{GF} - V_{ch}} + \dfrac{\left(X_{Deep}/\phi_{Deep}\right) + \left(X_{Tail}/\phi_{Tail}\right)}{X_{Deep} + X_{Tail}}} \quad V_{GF} > V_{ch}$$

$$\psi = V_{GF} \text{ when } V_{GF} < V_{ch} \tag{5.14}$$

The expression shown in Eq.(5.14) is a closed form expression for surface potential in a n-channel OTFT considering double exponential density of states. There is no special function or fitting parameters in this expression. All parameters are related to intrinsic material properties of the OTFT. The two cases in Eq.(5.14) signify the extent of band bending near the gate dielectric/channel interface. When the potential V_{GF} is small, there is only a little band bending and surface potential follows V_{GF}. But, when V_{GF} becomes significantly large, the extent of bending near the surface is determined by the distribution of the localized trap states. Here, the Fermi level moves closer to the LUMO edge filling more and more trap states which leads to increase in the charge carrier density. However, when all the trap states are filled, the surface potential can't increase further and finally saturates.

5.4 RESULTS AND DISCUSSION

To compare the accuracy of analytical expression derived in Eq.(5.14) we have implemented a numerical solver using MATLAB®. The numerical solver uses an iterative technique to calculate surface potential from Eq.(5.8). A numerical technique, bisection method, which uses two starting variables to iteratively arrive at the solution is used. Two variable starting method are preferred over single variable starting methods. The advantages of two variable starting methods include: (i) guaranteed

convergence: if proper choice of the initial guess is done, (ii) computational efficiency: they evaluate only one function per iteration unlike the other methods which may necessitate the computation of the function as well as its derivative and (iii) the error can be controlled. The choice of starting variables is important to ensure convergence. A necessary condition for obtaining a solution using bisection method is that the two starting values should lie on either side of the solution. The relative tolerance for this simulation is kept at 10^{-9} which ensures that the surface potential values obtained from the numerical solution are highly accurate. Such a tight relative tolerance value helps us to prove the accuracy of proposed analytical expression for surface potential. In general, relative tolerance can be set to 10^{-6} which is sufficient for a reasonable accuracy in calculating the surface potential. The surface potential values obtained using the numerical solver is shown in Fig.5-4. The parameters used for simulation are reported in Table-5.1 which are obtained from [16]. Surface potential values for varying V_{GF} (V_{GS}-V_{FB}) and V_{ch} are shown in Fig.5-4. As explained earlier, surface potential tends to follow V_{GF} at lower values and gradually saturates as V_{GF} increases.

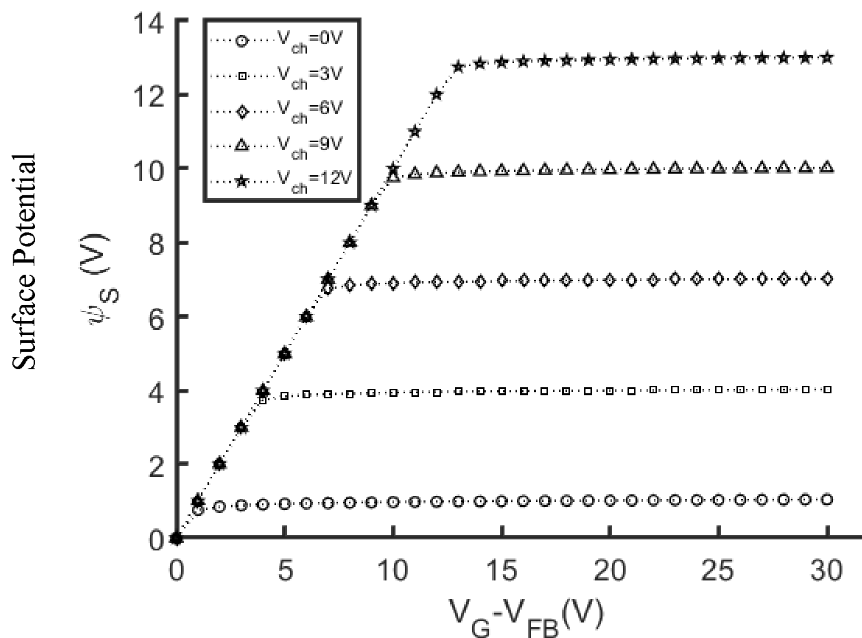

Figure 5-4 Variation of surface potential as a function of V_{GF} for various V_{ch}

A comparison between the numerical solution and analytical solution is shown in Fig.5-5. It can be observed that analytical solution matches with the numerical

solution. Error analysis is shown in Fig.5-6 where the absolute percentage error is plotted as a function of V_{GF}. The error is obtained by comparing surface potential obtained from analytical expression, with numerical solution. It is observed that the maximum absolute error is at 0.6% which is a very small value. After analyzing the absolute error at various values of V_{ch} we have observed that absolute error is always less than 1% which confirms the accuracy of our analytical solution. Also it is to be noted that the analytical solution is obtained in a single step. The solution has only simple algebraic operations which make it an appropriate choice to be incorporated in circuit simulators.

Table 5-1 Parameters used in the simulation [16]

Parameter	Value	Parameter	Value
N_{Deep}	$4.8\times10^{19}/cm^3$	ε_{osc}	$3\varepsilon_0$
N_{Tail}	$4.2\times10^{21}/cm^3$	C_i	17 nF/cm^2
ϕ_{Deep}	80 meV	E_{F0}	1eV
ϕ_{Tail}	30 meV	T	300K

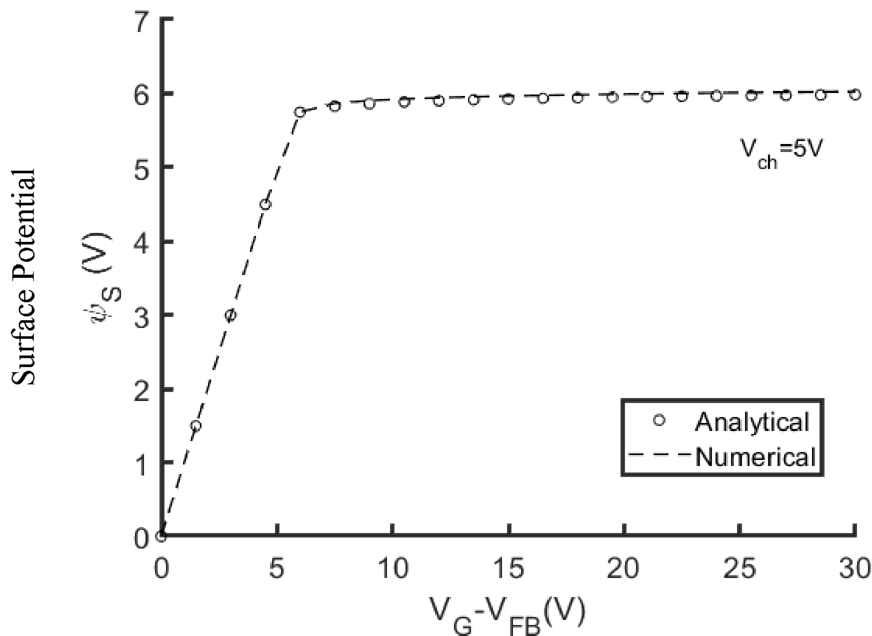

Figure 5-5 Comparison of surface potential obtained from analytical expression and numerical simulation.

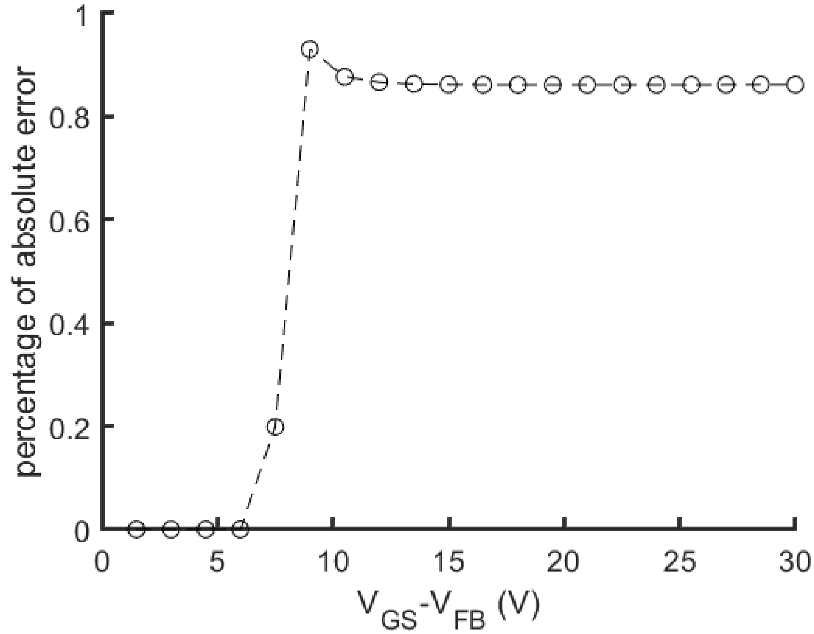

Figure 5-6 Percentage of absolute error in surface potential calculated from numerical solution and analytical expression as a function of V_{GF} at V_{ch}=7

Further, the I-V characteristics of an OTFT are obtained using the analytical expression derived for surface potential. For this we use, the all-region I-V characteristics equation shown in Eq.(5.15). [165]

$$I_D = \frac{W}{L}\mu C_i\left[V_{GS}(\psi_{source} - \psi_{Drain}) - \frac{1}{2}(\psi_{source}{}^2 - \psi_{Drain}{}^2)\right] \quad (5.15)$$

where, ψ_{source} and ψ_{Drain} represent the source and drain potentials respectively and calculated at source and drain ends of the OTFT. It is assumed that the contacts are ideal with no potential drop or contact resistance which is a valid assumption for long channel OTFTs operating with large voltages. The mobility value is also assumed to be $\mu = 1cm^2/V-s$ which is a valid approximation for an OTFT. In this case we intentionally neglected the dependence of mobility on various factors like electric field and gate to source potential (*V_{GS}*) to demonstrate the elegance of our surface potential expression in accurately modeling the drain current. A detailed explanation on various charge transport mechanisms in organic semiconductors and the mobility expressions

are elaborately discussed elsewhere [24], [38], [169] .The I_D Vs V_{DS} characteristic curves for an n-channel OTFT are shown in Fig.5-7. The I-V characteristics clearly show the linear and saturation regions of an OTFT and a smooth transition from linear to saturation region can also be seen. Fig.5-8 shows the I-V characteristics of a p-channel OTFT. In Fig.5-9 the output characteristics obtained using our model is compared with the experimental data [170] using a constant mobility. It is observed that there is a close match between the two. Slight deviations observed can be attributed to factors like the contact resistance, drain voltage dependence of mobility. In Fig.5-10, the experimental data [170] is fitted against our model but this time using a simple power law dependency of the mobility on the gate voltage. Using this model, it can be observed that I-V characteristics can be accurately modeled over a wide range of V_{SG} and V_{SD}.

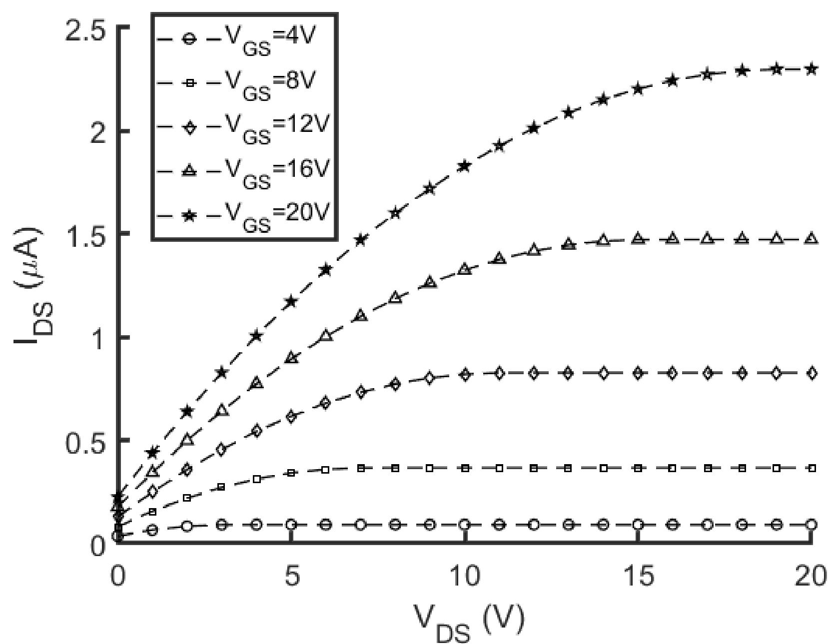

Figure 5-7 Normalized drain current I_{DS} as a function of V_{DS} and V_{GS} in an n-channel OTFT

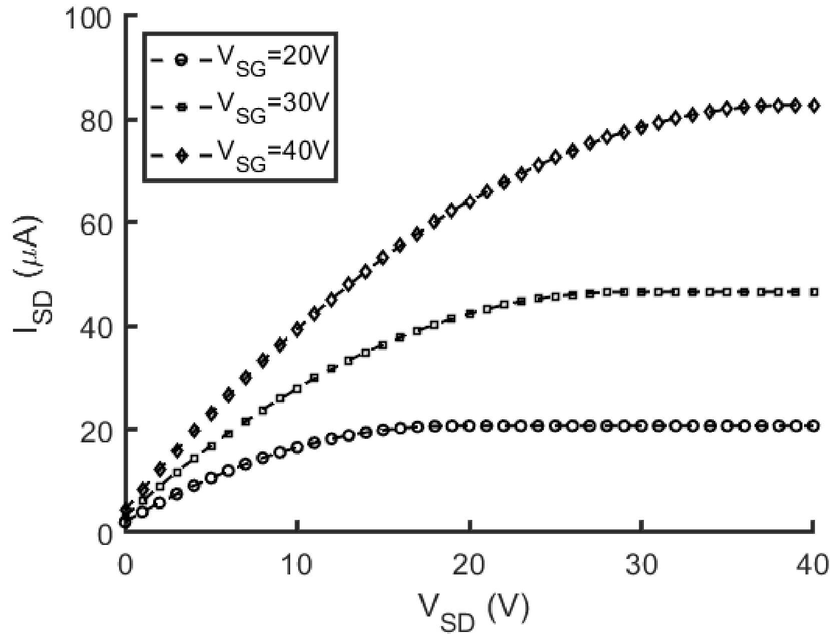

Figure 5-8 I_{SD} Vs V_{SD} as a function of V_{SG} for a p-channel OTFT based on our model to fit the experimental data provided in [170]. **μ=0.10 cm^2/Vs , W/L=50, C_i=11.5 nF/cm^2, N_{Deep}=4.2×10^{19} cm^{-3}eV^{-1}, N_{Tail}=3×10^{21} cm^{-3}eV^{-1}, ϕ_{Tail} = 18 meV, ϕ_{Deep} = 46 meV.**

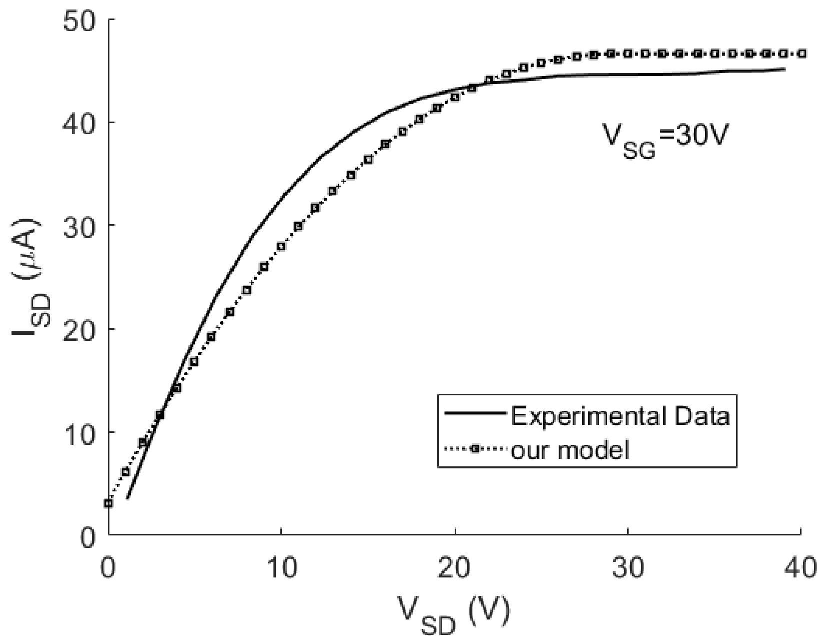

Figure 5-9 I_{SD} Vs V_{SD} at V_{SG}=30V using a constant mobility model. μ=0.10 cm^2/Vs, W/L=50, c_{ox}=11.5 nF/cm^2, N_{Deep}=4.2×10^{19} cm^{-3}eV^{-1}, N_{Tail}=3×10^{21} cm^{-3}eV^{-1}, ϕ_{Tail} = 18 meV, ϕ_{Deep} = 46 meV. Experimental data from [170]

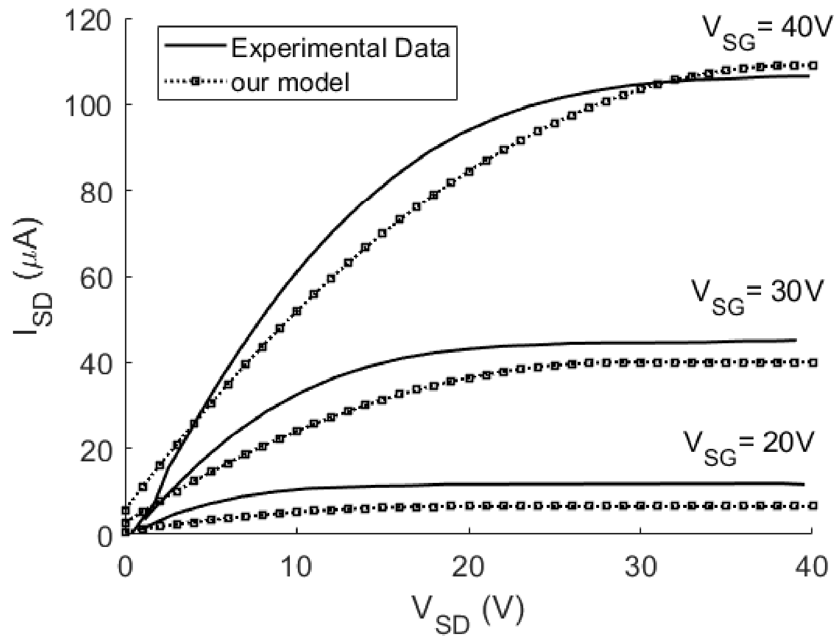

Figure 5-10 I_{SD} Vs V_{SD} for various V_{SG}: comparison of our model (symbols) with experimental data (solid lines) [170] **using a simple power law mobility model $\mu=\mu_0\times(V_{SG}-V_{T0})^{\alpha}$. μ_0= 0.02 cm^2/Vs, α=0.78, V_{T0}=16.2V.**

Through a simple yet accurate formulation for surface potential, we presented a model for drain current in OTFTs. This model is a suitable model for circuit simulators because of its algebraic simplicity and non-iterative nature. Although a few assumptions are made while deriving I-V characteristics, the model suits well for long channel OTFTs in its present form. It would be interesting to see how contact effects like injection barrier at the source/drain contacts, position of the contact terminals like top/bottom and length of the contacts could be incorporated in this model. A comprehensive investigation on how the surface potential alters with these physical parameters could be an interesting topic. Moreover, this model is developed considering the gradual channel approximation which assumes the channel length is fairly large. Therefore, how well the model scales for short channel OTFTs and what modifications are required for this model to incorporate various short channel effects could be another interesting aspect. However, the model presented in this work is quiet suitable for modeling OTFTs for a majority of applications like display driver circuits, sensors and RFID tags which uses long channel OTFTs.

5.5 CONCLUSION

Surface potential based models are an appropriate choice for developing an accurate and physics based model for an OTFT. This work addresses the problem of computing surface potential in an OTFT whose trap state density is molded using the double exponential density of states function. The existing techniques, either employ an iterative method or some special mathematical function. Both these approaches fit poorly into the circuit simulation tools. Therefore, a single analytical solution, without using any special functions is presented in this work. This expression is highly accurate: computes the surface potential with an accuracy up to a few nano-Volts, computationally efficient: single step process, which involves simple algebraic expressions. Moreover, it is a physics based model without any empirical constants or fitting parameters. Hence, this model is a suitable one for incorporating into circuit simulators which can be used to design and optimize OTFT based circuits.